Desalination and Water Treatment
www.deswater.com

doi: 10.5004/dwt.2017.20589

74 (2017) 269–277
May

Removal of phenol from aqueous solution using persulfate activated with nanoscale zero-valent iron

Müslün Sara Tunç*, Ozlem Tepe

Department of Environmental Engineering, Faculty of Engineering, Fırat University, 23119 Elazig, Turkey,
Tel. +90 424 2370000-5610; Fax: +90 424 2415526; emails: saratunc@firat.edu.tr (M.S. Tunç), otepe@firat.edu.tr (O. Tepe)

Received 16 June 2016; Accepted 8 February 2017

ABSTRACT

In this study, the removal of phenol by persulfate (PS) activated with nanoscale zero-valent iron (nZVI) was investigated. The influence of operation parameters such as pH, nZVI dosage, PS concentration and the initial phenol concentration on the phenol removal was evaluated through a series of batch experiments. The generated nZVI particles were characterized by Fourier transform infrared spectrophotometer, X-ray diffraction, scanning electron microscopy and Brunauer–Emmett–Teller analyses. The combination of nZVI and PS was more effective for the removal of phenol in comparison to nZVI alone and PS alone. Phenol removal enhanced with increase of nZVI dosage from 0.1 to 0.4 g/L and PS concentration from 5 to 12.5 mM. Phenol and chemical oxygen demand (COD) removal decreased with increase of the initial phenol concentration. Phenol and COD removal of 92.4% and 61.3% were obtained under the following conditions: natural pH of solution, nZVI dosage of 0.4 g/L, PS concentration of 10 mM and phenol concentration of 50 mg/L. The first-order kinetics was applied to the data. It was found that phenol removal by combination of nZVI and PS fitted first-order kinetics. Radical quenching studies revealed that the dominant radical species was sulfate radicals ($SO_4^{\bullet-}$). The findings showed that the combination of nZVI and PS could be effective for phenol removal.

Keywords: Nanoscale zero-valent iron; Persulfate; Phenol removal; Sulfate radical

---

1. Introduction

Industrial processes generate various compounds that may cause water and air pollution and have negative impacts for ecosystems and humans because of toxicity, carcinogenic and mutagenic properties. One of the most common organic water pollutants generated by the industrial processes is phenol [1]. Phenols are commonly used to produce various resins that include phenolic resins, which are used as construction materials for automobiles and appliances, epoxy resins and adhesives, and polyamide for various applications [2]. Wastewaters from various industries such as refineries, coking operations, coal processing, pharmaceuticals, plastics, wood products, pesticide, paint, paper and phenol production industries contain phenolic compounds [2,3].

When wastewater containing phenol discharges into water bodies, they hinder the growth and reproduction of aquatic life, endanger agriculture and also threaten to human health [4]. Drinking water contaminated by phenol may induce protein degeneration, tissue erosion, and paralysis of the central nervous system as well as damaging the kidney, liver and pancreas in human bodies [5]. Phenolics are toxic to fish even at a level of 1–2 mg/L and to most of the aquatic organisms in the range of 10–100 mg/L [6]. Phenols are considered as priority pollutants and have been classified as hazardous pollutants because of potential effects mentioned above [2]. In order to avoid the negative impacts of phenols on the environment, wastewaters containing this toxic compound must be treated effectively before they are discharged into the environment [7].

Various treatment technologies such as biological treatment [7], adsorption [8], advanced oxidation [9] and membrane processes [10] have been used to remove phenols

---

* Corresponding author.

1944-3994/1944-3986

from wastewater. Among these technologies, advanced oxidation processes (AOPs) are an attractive alternative for treating wastewater containing non-biodegradable organic pollutants [3] and have received considerable attention recently [11].

In literature, it is reported that Fenton-based homogeneous AOPs such as Fenton, photo-Fenton, electro-Fenton and photoelectro-Fenton have been used for the degradation of various organic pollutants [6,12–17]. These methods generate hydroxyl radicals which are reactive intermediates and have high oxidation potential [3]. However, there are several drawbacks associated with homogeneous Fenton processes. These include the requirement of further treatments for iron ions and sludge, acidification of effluents before removal of contaminant and neutralization of treated effluents before disposal [18]. To overcome these drawbacks, heterogeneous Fenton-like processes utilizing iron-based catalysts such as zero-valent iron (ZVI; Fe^0) [19,20], nanoscale zero-valent iron (nZVI) [18,21,22] and Fe_3O_4 [4,23] have been developed in recent years.

ZVI has been commonly used for removal of various pollutants such as chlorinated hydrocarbons, nitrobenzenes, chlorinated phenols, polychlorinated biphenyls, heavy metals and various anions because of its low cost and strong redox potential. nZVI (nano-Fe^0) displays a higher activity than bulk ZVI in reduction reactions owing to its high specific surface area and surface reactivity [24].

In AOPs, persulfate (PS; $S_2O_8^{2-}$) ($E^0 = 2.01$ V) has appeared as an alternative oxidant in recent years since its activation leads to the formation of strongly oxidizing sulfate free radicals ($SO_4^{\bullet-}$, $E^0 = 2.6$ V). It possesses higher redox potential than H_2O_2 ($E^0 = 1.76$ V) [11,25]. It has several advantages which include high solubility in water, non-selectively reactivity, relative stability at room temperature, widespread reactivity with environmental contaminants and high stability in aqueous systems [26]. In addition to these, it has ease of storage and transport, relatively low cost [27] and wide operative pH range [25]. The PS anion is activated by heat, transition metal ions and UV light to generate the sulfate free radical ($SO_4^{\bullet-}$), which is a stronger oxidant than PS anion as described in the following reactions [26,28].

$$S_2O_8^{2-} + \text{heat/UV} \rightarrow 2SO_4^{\bullet-} \tag{1}$$

$$S_2O_8^{2-} + Me^{n+} \rightarrow SO_4^{\bullet-} + Me^{(n+1)+} + SO_4^{2-} \tag{2}$$

Additionally, the presence of $SO_4^{\bullet-}$ in the aqueous solution can lead to formation of hydroxyl radial ($OH^\bullet$) via radical interconversion reactions by the following reactions [29].

All pHs:

$$SO_4^{\bullet-} + H_2O \rightarrow SO_4^{2-} + OH^\bullet + H^+ \tag{3}$$

Alkaline pH:

$$SO_4^{\bullet-} + OH^- \rightarrow SO_4^{2-} + OH^\bullet \tag{4}$$

Among transition metal ions, ferrous ions are the most widely used as activator for the activation of PS. The generally accepted mechanism for ferrous ions activating PS involves the following steps [25]:

$$S_2O_8^{2-} + Fe^{2+} \rightarrow SO_4^{\bullet-} + SO_4^{2-} + Fe^3 \tag{5}$$

$$SO_4^{\bullet-} + Fe^{2+} \rightarrow SO_4^{2-} + Fe^{3+} \tag{6}$$

Several studies have been carried out by combination of ZVI and PS for the degradation of organic pollutants including 2,4-dichlorophenol [25], *p*-chloroaniline [26], naphthalene [30], 4-chlorophenol [31], trichloroethylene [32], polyvinyl alcohol [28], 2,4-dinitrotoluene [33] and dyes [34,35], and these studies demonstrated that the combination of ZVI and PS is effective for the degradation of organic compounds. The objective of this study was to investigate the removal of phenol in the presence of nZVI and PS via batch experiments. Moreover, the influence of operating parameters such as initial pH, nZVI dosage, PS concentration and initial pollutant concentration on the removal of phenol was evaluated and radical quenching studies were performed to detect dominant radical species generated in the nZVI/PS system.

2. Materials and methods

2.1. Chemicals

Ferric chloride hexahydrate ($FeCl_3 \cdot 6H_2O$) was purchased from Carlo Erba (France). Sodium borohydride, potassium persulfate ($K_2S_2O_8$), phenol and *tert*-butyl alcohol (TBA) were purchased from Merck (Germany). Ethanol was purchased from Sigma-Aldrich (USA). All the chemicals used in this study were of analytical grade and used as received from the supplier. All solutions were prepared with distilled water. nZVI was produced in the laboratory using ferric chloride hexahydrate and sodium borohydride.

2.2. Synthesis and characterization of nanoscale ZVI particles

Synthesis of nZVI particles used in this study was carried out by using the borohydride reduction method according to Hwang et al. [36]. nZVI was prepared in a 500-mL flask reactor with four open necks in the laboratory. The central neck was housed with a tunable mechanical stirrer and the solution was stirred vigorously (250 rpm). To reduce ferric ions to nZVI, 250 mL of borohydride solution (358.5 mM BH_4^-) was introduced with a constant delivery rate of 20 mL/min into 250 mL of ferric ion (Fe^{3+}) solution (71.7 mM Fe^{3+}) from one of the necks on side of the flask reactor. Other two necks were used for the inlet and outlet of nitrogen gas to prevent any possible oxidation of iron. The reduction reaction is described as follows:

$$4Fe^{3+} + 3BH_4^- + 9H_2O \rightarrow 4Fe^0 + 3H_2BO_3^- + 12H^+ + 6H_2 \tag{7}$$

The generated black nZVI particles were collected by vacuum filtration of the solution after a 20 min of aging period. The collected particles were then washed three times with ethanol, and dried in an oxygen-free chamber for instant usage.

The generated nZVI particles were characterized by Fourier transform infrared spectrophotometer (FTIR), X-ray diffraction (XRD), scanning electron microscopy (SEM) with energy dispersive X-ray (EDX) and Brunauer–Emmett–Teller (BET) analyses. The multipoint BET surface area was determined with Micromeritics Gemini 2360. XRD patterns were obtained using an X-ray diffractometer (Bruker D8 Advance) with Cu Kα radiation, operated at 40 kV and 40 mA. Scans were recorded with diffraction angles ranging from 5° to 90° 2θ. FTIR spectra of nZVI were obtained between 400 and 4,000 cm^{-1} using FTIR spectrometer (ATI Unicam Mattson 1000). The surface structures and sizes of nZVI particles were analyzed by SEM (JEOL JSM 7001F) at voltage of 15 kV.

2.3. Experimental procedure

Batch experiments were performed in 250-mL Erlenmeyer flasks with 100 mL of aqueous solution. The pH of the solutions was adjusted by adding diluted H_2SO_4 or NaOH using a pH meter (Orion 3 STAR). The experiments were carried out in an orbital shaker (Gallenkamp) at a constant temperature (25°C) and 160 rpm shaking speed. Phenol solutions were prepared by diluting a stock phenol solution of 1 g/L. Samples withdrawn at different time intervals were centrifuged at 5,000 rpm for 5 min using a centrifuge (Nüve NF 800R) and analyzed for determining phenol concentration. Radical quenching experiments were performed to identify the dominant radical oxidizing species responsible for phenol removal in the nZVI/PS system. In the study, ethanol (EtOH) and TBA were used as radical scavengers at various molar ratios of scavenger to phenol. Control tests in the absence of nZVI and PS were also conducted and it was observed that phenol concentration did not change during reaction.

2.4. Analysis

The concentration of phenol in aqueous solutions was determined spectrophotometrically using an UV–Vis Spectrophotometer (Perkin-Elmer Lambda 25). The absorbance of the colored complex of phenol with *p*-nitroaniline was read at 470 nm [37]. The removal efficiency of phenol and COD, *R* (%), was calculated using the following equation:

$$R(\%) = \frac{C_0 - C_t}{C_0} \times 100 \tag{8}$$

where R (%) represented the phenol or COD removal efficiency, C_0 (mg/L) and C_t (mg/L) were the initial concentration of phenol or COD in the solution and concentration of phenol or COD at t min. COD was determined by open reflux method described in Standard Methods for Examination of Water and Wastewater [38].

3. Results and discussion

3.1. Characterization of nZVI

The specific surface area of the synthesized nZVI was determined to be 60 m^2/g. The XRD pattern of the synthesized nZVI particles is presented in Fig. 1. The characteristic peak observed at the 2θ angle of 44.72° showed the existence of ZVI. The broad iron peak signified that the synthesized nZVI particles had an amorphous structure [39,40]. A similar result was obtained by Fang et al. [40] and Fan et al. [41].

Surface morphology of nZVI is a significant characteristic that may affect the performance of nanoparticles in heterogeneous Fenton oxidation [25]. The surface morphology and elemental composition of nZVI before and after the reaction were investigated by an SEM–EDX and are presented in Figs. 2(a) and (b). As seen from SEM images, the nZVI particles had spherical morphology and chain-like structures. The sizes of nZVI particles were mostly in the range of 40–100 nm. The chain-like structures may have arisen from both the influences of the static magnetism and surface tension. These chain-like structures were also observed by several researchers [6,25,40,42,43]. However, after nZVI was used as a catalyst, the chain-like aggregates were damaged and large space structures were observed owing to the corrosion of nZVI in the aqueous solution as shown in Fig. 2(b). According to EDX analysis, nZVI was composed of 89% iron and 11% oxygen before the reaction. The oxygen element after the reaction increased while Fe decreased. This indicated that nZVI was oxidized to Fe^{2+}, and Fe^{2+} was leached from the iron oxides on the nZVI surface since some iron oxide was formed [25]. Additionally, the C element observed after the reaction indicated that phenol or its intermediates were absorbed onto the nZVI surface. Considering these results, it may be stated that nZVI particles are not only a source of Fe^{2+}, but they also have an absorption potential [25].

FTIR analysis gives information about the spectra of carboxyl, carbonyl, hydroxyl, amino and other functional groups, as well as double and triple bonds [44]. FTIR spectra of nZVI before and after the reaction are presented in Fig. 3. The several absorption peaks appeared after the reaction. The bands at 3,548, 3,469, 3,413 and 3,242 cm^{-1} were ascribed to O–H stretching vibration. The peak at 1,486 cm^{-1} displayed C=C vibration band for aromatic rings. The band observed at 1,617 cm^{-1} was related to C=C stretching and N–H bending vibration. The appearance of bands at 1,096 and 1,008 cm^{-1} represented the C–O stretching vibration. These can be attributed to intermediates of phenol after the reaction. The peaks at 1,384, 829 and 755 cm^{-1} represented C–H bending vibration of aliphatic compounds. Similarly, the band observed at 2,927 cm^{-1} indicated C–H stretching vibration. Furthermore, the bands observed at 621, 473 and 416 cm^{-1} corresponded to Fe–O stretch of Fe_2O_3 and Fe_3O_4. This shows that nZVI was oxidized as described in SEM–EDX analysis.

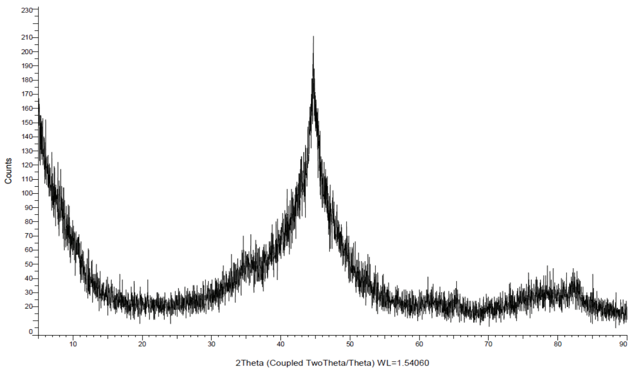

Fig. 1. XRD pattern of the synthesized nZVI.

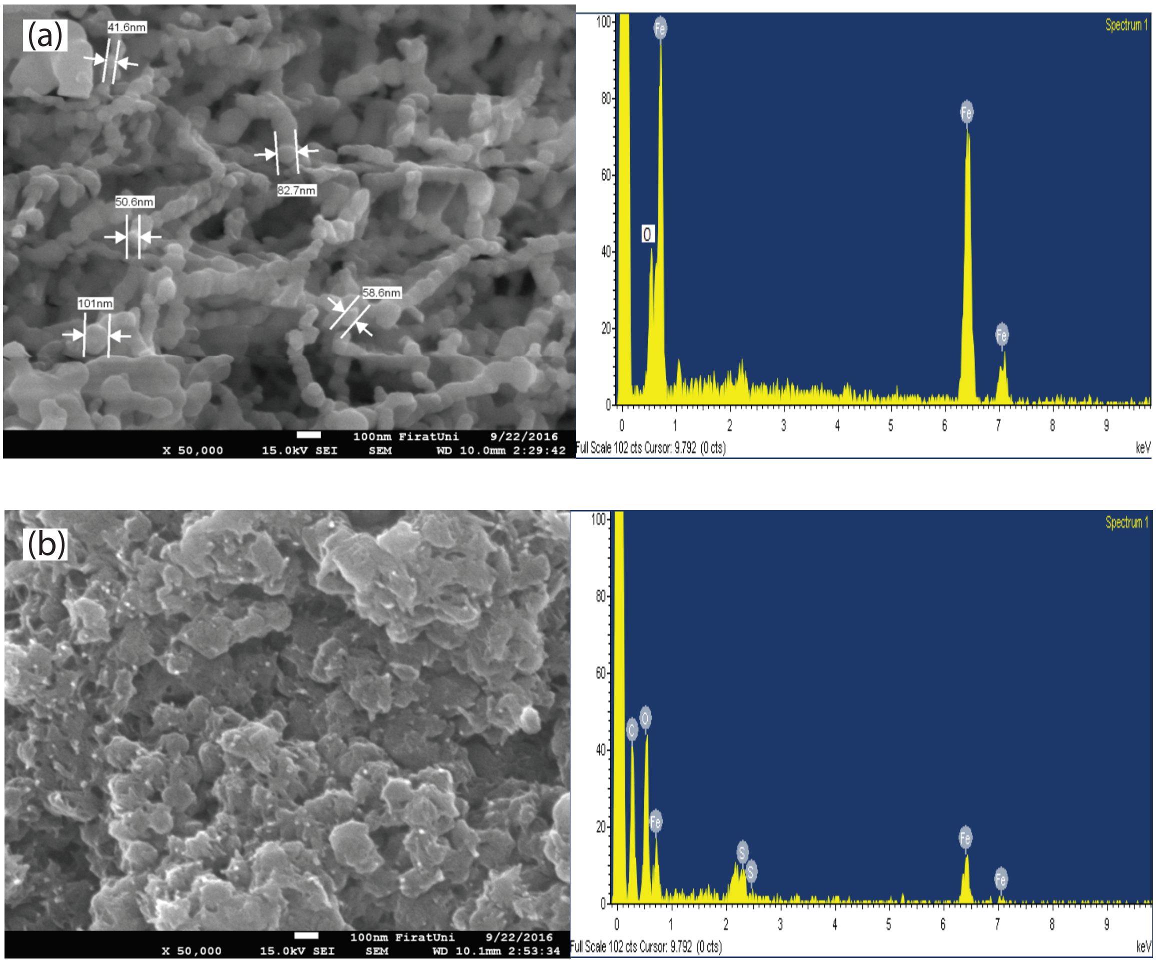

Fig. 2. SEM images of nZVI before (a) and after reaction (b).

3.2. *Removal of phenol using different systems*

In order to investigate the removal of phenol by nZVI alone, PS alone and the combination of nZVI and PS, the experiments were performed using the solutions with 50 mg/L phenol concentration at an initial pH of 5.85 (natural pH of solution) and the results are given in Fig. 4. As seen in Fig. 4, the removal efficiencies of phenol obtained by nZVI alone and PS alone were 8.9% and 10.7%, respectively, after the reaction time of 180 min. This result showed that no significant phenol removal was achieved by nZVI alone and PS alone. The removal of phenol by nZVI alone was because of reduction or adsorption on the nZVI surface. In PS system alone, phenol has been removed via reduction [26]. The removal efficiency of phenol increased to 40.6% when 0.5 g/L nZVI was used in the presence of 10 mM PS. The usage of nZVI with PS resulted in more rapid and effective removal of phenol in comparison to nZVI alone and PS alone. This was attributed to the formation of sulfate free radicals having high oxidation potential because of the activation of PS with nZVI [26]. Similar findings are available in the literature. Zhao et al. [31] observed no significant degradation of 4-chlorophenol in the presence of ZVI alone and PS alone. However, they obtained effective degradation of 4-cholorophenol by PS activated with ZVI.

3.3. *Influence of initial pH*

It is well known that pH is a critical parameter, which influences the performance of all chemical processes of wastewater treatment [45]. The value of pH influences the dissolution of Fe(II) from nZVI strongly, which affects the rate and mechanism of phenol degradation [25]. The influence of initial pH on the removal of phenol by the nZVI/PS system was investigated at five different pH values (2, 3, 4, 5 and 5.85 (natural pH of solution)). Fig. 5 depicts the influence of initial pH on the removal of phenol at 10 mM PS concentration and 0.5 g/L nZVI dosage. When the initial pH of the phenol solution was 2, 3, 4, 5 and 5.85, the phenol removal efficiencies were obtained as 48%, 48%, 34.5%, 36.6% and 40%, respectively, after the reaction time of 180 min. As shown in Fig. 5, phenol removal relatively rose with the decrease of the solution pH and the highest removal efficiency was achieved to be 48% at pH values of 2 and 3. ZVI is oxidized to ferrous ion (Fe^{2+}) at acidic conditions. Thus, ferrous ion is introduced significantly to solution at pH values of 2 and 3 [45]. Many studies indicated that acidic condition was more favorable for degradation of organic compounds by PS activated with ZVI when compared with alkaline conditions [26,27]. Fe^{2+} is more easily released to solution from the nZVI surface when

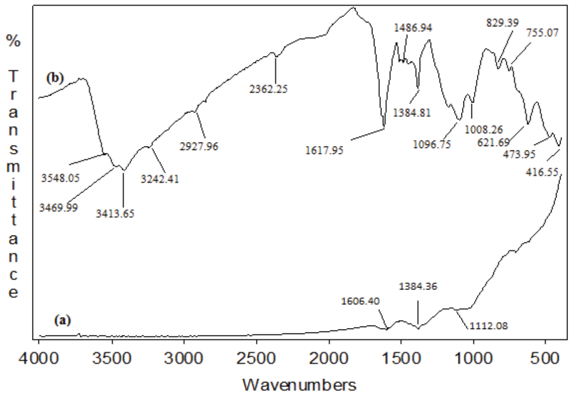

Fig. 3. FTIR spectra of nZVI before (a) and after reaction (b).

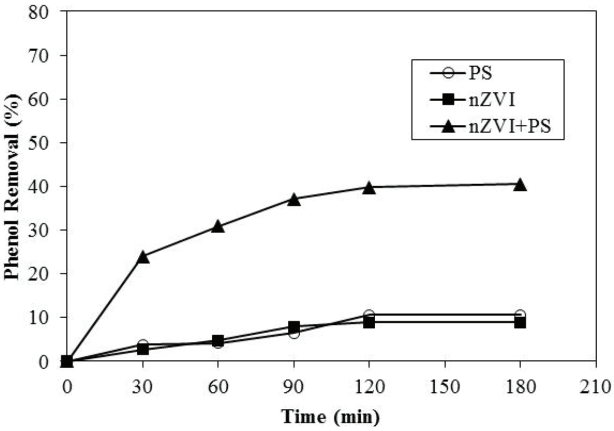

Fig. 4. Comparison of phenol removal using different systems (experimental conditions: nZVI = 0.5 g/L, PS = 10 mM, initial phenol concentration = 50 mg/L and no pH adjustment).

the value of pH is below 4.0. However, the precipitation of Fe^{3+} occurred when the pH was higher than 4.0, leading to the adsorption of iron hydroxides onto surface of nZVI, and consequently formed electronic barriers, which inhibited the corrosion of nZVI and the release of Fe^{2+} [25]. On the other hand, the natural pH of the solution (pH 5.85) without pH adjustment provided phenol removal of 40%. This result suggests that low solution pH slightly improves phenol removal. Since differences among removal efficiencies of phenol at the pH values tested in this study were insignificant, the following experiments were performed without pH adjustment. Zhao et al. [31] stated that the optimum pH for the highest degradation efficiency of 4-cholorophenol by ZVI and peroxydisulfate system was 6.0.

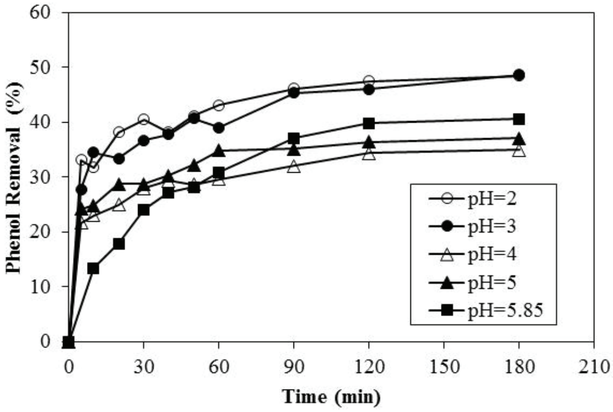

Fig. 5. The effect of pH on phenol removal (experimental conditions: nZVI = 0.5 g/L, PS = 10 mM, initial phenol concentration = 50 mg/L).

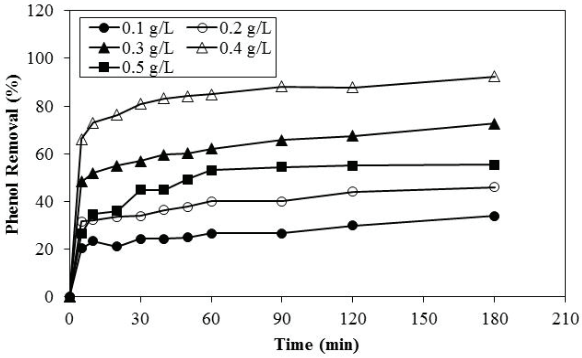

Fig. 6. The effect of nZVI dosage on phenol removal (experimental conditions: PS = 10 mM, initial phenol concentration = 50 mg/L and no pH adjustment).

3.4. Influence of nZVI dosage

The influence of nZVI dosage on the removal of phenol in the nZVI/PS system was investigated in the range of 0–0.5 g/L using phenol concentration of 50 mg/L at 10 mM PS and natural pH of the solution (pH 5.85), and the results are depicted in Fig. 6. As described above, in the presence of PS alone without nZVI, no significant removal of phenol (10.7%) was observed after the reaction time of 180 min. As it can be seen in Fig. 6, when the dosage of nZVI was increased from 0.1 to 0.4 g/L, phenol removal efficiency increased from 33.4% to 92.4% after the reaction time of 180 min, respectively. According to the literature, it is clear that ZVI plays a role of source of Fe^{2+} which is one of the main species that can activate PS to produce sulfate free radicals (SO$_4^{\bullet-}$) and the existence of Fe^{2+} can significantly influence the efficiency of contaminant removal [26,27]. However, phenol removal decreased when the nZVI dosage of 0.5 g/L was used. This may be due to agglomeration of nZVI particles [21] and scavenging of sulfate radicals. Fe^{2+} can act as a sulfate scavenger radical at high Fe^{2+} concentration as described in reaction (6) [27].

Similar results have been reported in other studies about the degradation of pollutants by PS activated with ZVI [27]. The optimum nZVI dosage to achieve the highest removal efficiencies of phenol was found as 0.4 g/L in this study. Therefore, this dosage was used in the further experiments.

Fig. 7 depicts the removal efficiencies of phenol and COD during the reaction time of 180 min at different nZVI dosages. As it can be seen in Fig. 7, the highest phenol and COD removal efficiencies were obtained as 92.4% and 61.3% at the nZVI dosage of 0.4 g/L. Both phenol and COD removal increased when nZVI dosage was raised from 0.2 to 0.4 g/L. At the nZVI dosage of 0.5 g/L, they both decreased. Phenol removal was higher than COD removal at all the nZVI dosages tested. This indicated that phenol did not completely mineralize into CO_2 and H_2O, and transformed to organic intermediates. Intermediates can be formed through the oxidation of organic pollutants in oxidation processes [45].

It was reported in the literatures that first-order kinetics have been applied for heterogeneous Fenton systems [18,21,45]. Considering these references, first-order kinetics equation given below was used for fitting the data in this study.

$$C = C_0 \exp(-k\,t) \tag{9}$$

where C_0 is the initial concentration of phenol, C is the concentration of phenol at time t and k is the reaction rate constant. k can be determined from the slope of the line in the plots of $\ln(C_0/C)$ vs. time.

The values of the first-order rate constants (k) and corresponding correlation coefficients (R^2) for phenol removal by nZVI/PS are given in Table 1. The high values of the correlation coefficient (R^2) showed that the removal of phenol by nZVI and PS fitted to first-order kinetics model. The values of the first-order rate constants (k) determined at nZVI dosages of 0.1, 0.2, 0.3, 0.4 and 0.5 g/L without pH adjustment were 0.0010, 0.0014, 0.0034, 0.0135 and 0.0022 min^{-1}, respectively. As it can be seen from Table 1, the values of the first-order rate constants increased with increasing of the nZVI dosage from 0.1 to 0.4 g/L, but the first-order rate constant decreased at the nZVI dosage of 0.5 g/L.

3.5. Influence of PS concentration

In the nZVI/PS system, PS produces sulfate free radicals, which are stronger oxidants than PS anion. The influence of PS concentration on phenol removal by the nZVI/PS system was investigated by varying PS concentration from 5 to 12.5 mM and the obtained results are shown in Fig. 8. As seen in Fig. 8, at the low PS concentration of 5 mM, the phenol removal efficiency was quite low. This may be due to insufficient sulfate free radicals in the aqueous solution. As the PS concentration was increased from 5 to 10 mM, phenol removal efficiency increased from 16.8% to 92.4% after the reaction time of 180 min. This situation may be because of higher levels of formation of sulfate free radicals. However, at a higher concentration (12.5 mM), no significant additional improvement was observed. Since the nZVI dosage was fixed, the amount of available sulfate free radicals was limited [25]. According to these results, following experiments were conducted using a PS concentration of 10 mM.

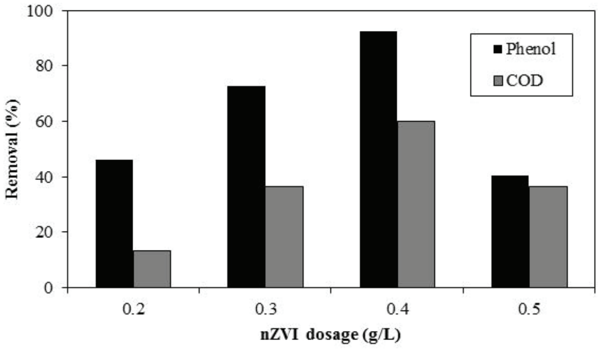

Fig. 7. The comparison of phenol and COD removal obtained on different nZVI dosages (experimental conditions: PS = 10 mM, initial phenol concentration = 50 mg/L, reaction time = 180 min and no pH adjustment).

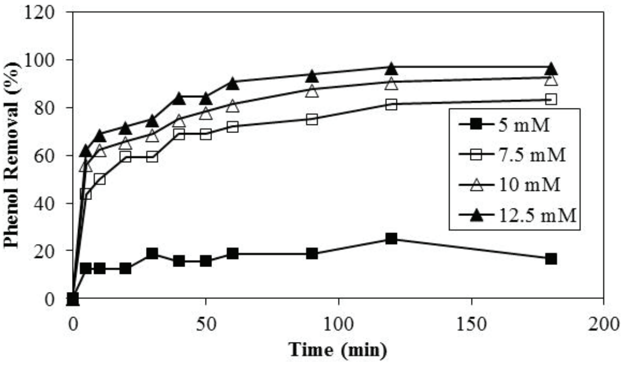

Fig. 8. The effect of PS dosage on phenol removal (experimental conditions: nZVI = 0.4 g/L, initial phenol concentration = 50 mg/L and no pH adjustment).

Table 1
Values of first-order rate constants (k) and corresponding correlation coefficients (R^2) for phenol removal by nZVI and persulfate

nZVI dosage (g/L)	PS concentration, mM	C_0 (phenol, mg/L)	k (min^{-1})	R^2
0.1	10	50	0.0010	0.9430
0.2	10	50	0.0014	0.9340
0.3	10	50	0.0034	0.9539
0.4	10	50	0.0135	0.9911
0.5	10	50	0.0022	0.8347
0.4	5	50	0.0012	0.8169
0.4	7.5	50	0.0088	0.9342
0.4	12.5	50	0.0216	0.9380

The comparison of phenol and COD removal obtained at different PS concentrations is shown in Fig. 9. With increase of PS concentration, both phenol and COD removal efficiencies increased. For example, phenol and COD removal were obtained as 16.8% and 12.9% at 5 mM PS concentration and 96.9% and 61.3% at 12.5 mM PS concentration, respectively, after the reaction time of 180 min. Like the results obtained at different nZVI dosages, phenol removal was higher than COD removal. As mentioned above, this situation may be attributed to formation of organic intermediates. As can be seen from Table 1, the removal rate of phenol by nZVI/PS followed this order of PS concentration of 12.5 mM > 10 mM > 7.5 mM > 5 mM with first-order rate constant (*k*) values of 0.0216, 0.0135, 0.0088 and 0.0012 min^{-1}, respectively.

3.6. Influence of initial phenol concentration

The influence of initial concentration of phenol on phenol removal was tested for three different concentrations in the range from 25 to 100 mg/L under the following conditions: natural pH of solution, 0.4 g nZVI/L and 10 mM PS, and the results are depicted in Fig. 10. When the initial concentration of phenol was increased from 25 to 100 mg/L, the phenol removal efficiency decreased from 100% to 65.2% after the reaction time of 180 min. The removal of phenol by nZVI is a heterogeneous process which includes both adsorption and degradation. Since the number of phenol molecules adsorbed on the surface of nZVI increase with an increase in initial concentration of phenol, this situation blocks the surface of nZVI and prevents further contact [3]. As a result of this, the generation of sulfate free radicals may be prevented and generated sulfate free radicals may be insufficient for removal of high concentrations of phenol. Therefore, the removal efficiency of phenol was low at high concentrations. COD removals obtained using nZVI and PS process were achieved as 61.3% and 28.3% after reaction time of 180 min at the initial phenol concentrations of 50 and 100 mg/L, respectively (not shown). Fig. 11 depicts the variation of phenol concentration and COD vs. time at the optimum condition. Phenol removal efficiency was higher than COD removal efficiency at all reaction times. Within the first 10 min of the reaction time, approximately 60% of phenol was removed while 4% of COD was removed. This result indicated that the majority of phenol was transformed into intermediates within the reaction time of 10 min. After the reaction time of 10 min, COD removal increased up to 61.3% in the reaction time of 120 min. It was stable after this time.

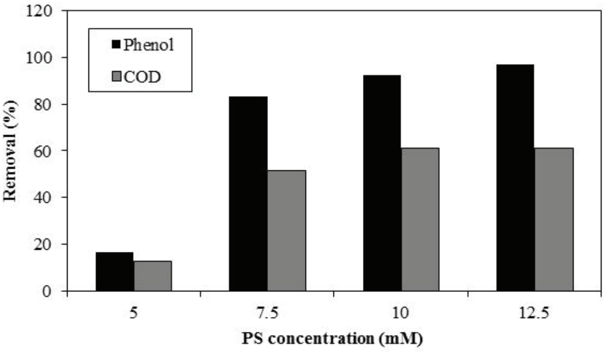

Fig. 9. The comparison of phenol and COD removal obtained on the different PS concentrations (experimental conditions: nZVI= 0.4 g/L, initial phenol concentration = 50 mg/L, reaction time = 180 min and no pH adjustment).

3.7. Free-radical quenching studies

In the literature, it was reported that alcohols with alpha hydrogen such as ethanol (EtOH) readily react with hydroxyl radicals and sulfate radicals while alcohols without alpha hydrogen such as TBA are effective quenching agents for hydroxyl radicals [31]. In order to evaluate the contribution of $SO_4^{\bullet-}$ and $OH^{\bullet}$ for phenol removal, EtOH and TBA were used as selective radical scavengers in this study. EtOH and TBA have been extensively used as radical scavengers in previous studies [46–48]. Phenol removal efficiencies in the presence of EtOH and TBA are depicted in Fig. 12. In the nZVI/PS system, $OH^{\bullet}$ can be identified by adding excess TBA while the contribution of $SO_4^{\bullet-}$ can be determined by considering the difference between phenol removal after spiking excess EtOH and TBA. As shown in Fig. 12, 92.4% of phenol was removed in the absence of radical quenching agents. However, phenol

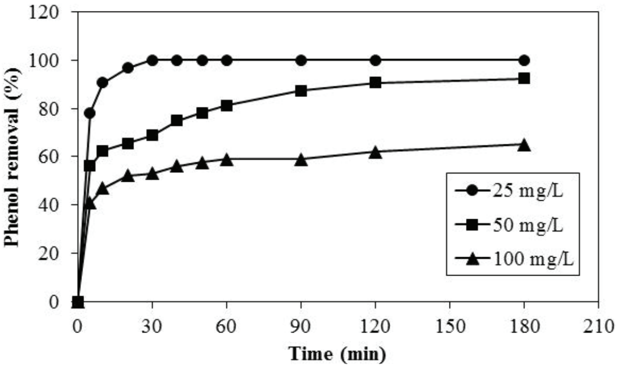

Fig. 10. The effect of initial phenol concentration on phenol removal (experimental conditions: nZVI = 0.4 g/L, PS = 10 mM and no pH adjustment).

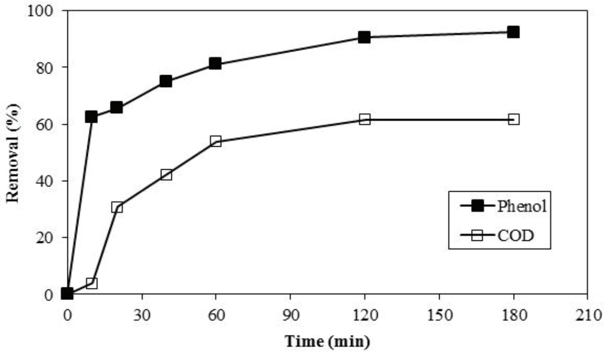

Fig. 11. The variation of phenol and COD removal vs. time on optimum condition (experimental conditions: nZVI = 0.4 g/L, PS = 10 mM, initial phenol concentration = 50 mg/L and no pH adjustment).

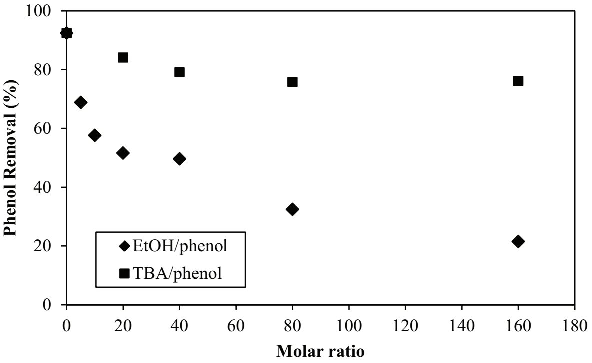

Fig. 12. Effect of radical scavengers on phenol removal (experimental conditions: nZVI = 0.4 g/L, PS = 10 mM, initial phenol concentration = 50 mg/L, reaction time = 180 min and no pH adjustment).

removal decreased in the presence of EtOH and TBA. The phenol removal efficiencies were about 84.0%, 79.1%, 76.1% and 76.1% at the molar ratios (TBA/phenol) of 20:1, 40:1, 80:1 and 160:1, respectively, while the efficiencies were about 68.8%, 57.6%, 51.6%, 49.6%, 32.4% and 21.5% at the molar ratios (EtOH/phenol) of 5:1, 10:1, 20:1, 40:1, 80:1 and 160:1, respectively. As it may be seen, phenol removal was significantly inhibited by adding EtOH as $OH^•$ radical and $SO_4^{•-}$ radical scavenger while it was quite a bit influenced by the addition of TBA as an effective quenching agent for hydroxyl radicals. From these results, it was evident that $SO_4^{•-}$ had a dominant role and $OH^•$ had a minor role for phenol removal. Consequently, the dominant radical species generated in the nZVI/PS system were sulfate radicals. Diao et al. [47] reported that dominant reactive species in a bentonite-supported nanoscale ZVI/PS system were $SO_4^{•-}$ radicals.

4. Conclusion

It was demonstrated that the combination of nZVI and PS was an efficient process for removal of phenol at the natural pH of solution. In the nZVI/PS system, nZVI not only supplied a high surface area and active sites, but also acted as a source of Fe^{2+} activating PS for generation of sulfate free radicals. 92.4% of phenol was removed within the reaction time of 180 min with the nZVI dosage of 0.4 g/L, the PS concentration of 10 mM and the initial phenol concentration of 50 mg/L at the natural pH of solution. Under the same condition, COD removal efficiency was found as 61.3%. The first-order kinetics was applied to the experimental data. It was found that phenol removal using nZVI and PS fitted to the first-order kinetics. $SO_4^{•-}$ radicals were identified as the dominant radical species responsible for phenol removal.

Acknowledgments

We thank Şeyda Taşar from Fırat University, Faculty of Engineering, Department of Chemistry Engineering, Elazig/Turkey for FTIR analyses.

References

[1] G. Busca, S. Berardinelli, C. Resini, L. Arrighi, Technologies for the removal of phenol from fluid streams: a short review of recent developments, J. Hazard. Mater., 160 (2008) 265–288.
[2] U.F. Alkaram, A.A. Mukhlis, A.H. Al-Dujaili, The removal of phenol from aqueous solutions by adsorption using surfactant-modified bentonite and kaolinite, J. Hazard. Mater., 169 (2009) 324–332.
[3] A. Babuponnusami, K. Muthukumar, Treatment of phenol-containing wastewater by photoelectro-Fenton method using supported nanoscale zero-valent iron, Environ. Sci. Pollut. Res., 20 (2013) 1596–1605.
[4] W. Wang, Y. Liu, T. Li, M. Zhou, Heterogeneous Fenton catalytic degradation of phenol based on controlled release of magnetic nanoparticles, Chem. Eng. J., 242 (2014) 1–9.
[5] H.B. Senturk, D. Ozdes, A. Gundogdu, C. Duran, M. Soylak, Removal of phenol from aqueous solutions by adsorption onto organomodified Tirebolu bentonite: equilibrium, kinetic and thermodynamic study, J. Hazard. Mater., 172 (2009) 353–362.
[6] A. Babuponnusami, K. Muthukumar, Advanced oxidation of phenol: a comparison between Fenton, electro-Fenton, sono-electro-Fenton and photo-electro-Fenton processes, Chem. Eng. J., 183 (2012) 1–9.
[7] G. Moussavi, M. Mahmoudi, B. Barikbin, Biological removal of phenol from strong wastewaters using a novel MSBR, Water Res., 43 (2009) 1295–1302.
[8] N. Massalha, A. Brenner, C. Sheindorf, Y. Haimov, I. Sabbah, Enriching composite hydrophilic polyurethane foams with PAC to enhance adsorption of phenol from aqueous solutions, Chem. Eng. J., 280 (2015) 283–292.
[9] H. Suzuki, S. Araki, H. Yamamoto, Evaluation of advanced oxidation processes (AOP) using O_3, UV, and TiO_2 for the degradation of phenol in water, J. Water Process Eng., 7 (2015) 54–60.
[10] A. Bódalo, J.L. Gómez, M. Gómez, G. León, A.M. Hidalgoa, M.A. Ruíza, Phenol removal from water by hybrid processes: study of the membrane process step, Desalination, 223 (2008) 323–329.
[11] J. Yan, M. Lei, L. Zhu, M.N. Anjum, J. Zou, H. Tang, Degradation of sulfamonomethoxine with Fe_3O_4 magnetic nanoparticles as heterogeneous activator of persulfate, J. Hazard. Mater., 186 (2011) 1398–1404.
[12] W.-P. Ting, M.-C. Lu, Y.-H. Huang, The reactor design and comparison of Fenton, electro-Fenton and photoelectro-Fenton processes for mineralization of benzene sulfonic acid (BSA), J. Hazard. Mater., 156 (2008) 421–427.
[13] W.-P. Ting, M.-C. Lu, Y.-H. Huang, Kinetics of 2,6-dimethylaniline degradation by electro-Fenton process, J. Hazard. Mater., 161 (2009) 1484–1490.
[14] D. Hermosilla, M. Cortijo, C.P. Huang, The role of iron on the degradation and mineralization of organic compounds using conventional Fenton and photo-Fenton processes, Chem. Eng. J., 155 (2009) 637–646.
[15] N. Masomboon, C. Ratanatamskul, M.-C. Lu, Kinetics of 2,6-dimethylaniline oxidation by various Fenton processes, J. Hazard. Mater., 192 (2011) 347–353.
[16] A. Babuponnusami, K. Muthukumar, Degradation of phenol in aqueous solution by Fenton, sono-Fenton and sono-photo-Fenton methods, Clean Soil Air Water, 39 (2011) 142–147.
[17] M.D.G. de Luna, J.I. Colades, C.-C. Su, M.-C. Lu, Comparison of dimethyl sulfoxide degradation by different Fenton processes, Chem. Eng. J., 232 (2013) 418–424.
[18] L. Xu, J. Wang, A heterogeneous Fenton-like system with nanoparticulate zero-valent iron for removal of 4-chloro-3-methyl phenol, J. Hazard. Mater., 186 (2011) 256–264.
[19] D.H. Bremner, A.E. Burgess, D. Houllemare, K.C. Namkung, Phenol degradation using hydroxyl radicals generated from zero-valent iron and hydrogen peroxide, Appl. Catal., B, 63 (2006) 15–19.
[20] T. Zhou, Y. Li, J. Ji, F.-S. Wong, X. Lu, Oxidation of 4-chlorophenol in a heterogeneous zero valent iron/H_2O_2 Fenton-like system: kinetic, pathway and effect factors, Sep. Purif. Technol., 62 (2008) 551–558.

[21] A. Babuponnusami, K. Muthukumar, Removal of phenol by heterogenous photo electro Fenton-like process using nano-zero valent iron, Sep. Purif. Technol., 98 (2012) 130–135.
[22] S. Zha, Y. Cheng, Y. Gao, Z. Chen, M. Megharaj, R. Naidu, Nanoscale zero-valent iron as a catalyst for heterogeneous Fenton oxidation of amoxicillin, Chem. Eng. J., 255 (2014) 141–148.
[23] S. Zhang, X. Zhao, H. Niu, Y. Shi, Y. Cai, G. Jiang, Superparamagnetic Fe_3O_4 nanoparticles as catalysts for the catalytic oxidation of phenolic and aniline compounds, J. Hazard. Mater., 167 (2009) 560–566.
[24] Y. Wang, H. Sun, X. Duan, H.M. Ang, M.O. Tade, S. Wang, A new magnetic nano zero-valent iron encapsulated in carbon spheres for oxidative degradation of phenol, Appl. Catal., B, 172–173 (2015) 73–81.
[25] R. Li, X. Jin, M. Megharaj, R. Naidu, Z. Chen, Heterogeneous Fenton oxidation of 2,4-dichlorophenol using iron-based nanoparticles and persulfate system, Chem. Eng. J., 264 (2015) 587–594.
[26] I. Hussain, Y. Zhang, S. Huang, X. Du, Degradation of *p*-chloroaniline by persulfate activated with zero-valent iron, Chem. Eng. J., 203 (2012) 269–276.
[27] X.-R. Xu, X.-Z. Li, Degradation of azo dye Orange G in aqueous solutions by persulfate with ferrous ion, Sep. Purif. Technol., 72 (2010) 105–111.
[28] S.-Y. Oh, H.-W. Kim, J.-M. Park, H.-S. Park, C. Yoon, Oxidation of polyvinyl alcohol by persulfate activated with heat, Fe^{2+}, and zero-valent iron, J. Hazard. Mater., 168 (2009) 346–351.
[29] C. Liang, Z.S. Wang, C.J. Bruell, Influence of pH on persulfate oxidation of TCE at ambient temperatures, Chemosphere, 66 (2007) 106–113.
[30] C. Liang, Y.-Y. Guo, Mass transfer and chemical oxidation of naphthalene particles with zero valent iron activated persulfate, Environ. Sci. Technol., 44 (2010) 8203–8208.
[31] J. Zhao, Y. Zhang, X. Quan, S. Chen, Enhanced oxidation of 4-chlorophenol using sulfate radicals generated from zero-valent iron and peroxydisulfate at ambient temperature, Sep. Purif. Technol., 71 (2010) 302–307.
[32] C. Liang, I.-L. Lee, In situ iron activated persulfate oxidative fluid sparging treatment of TCE contamination – a proof of concept study, J. Contam. Hydrol., 100 (2008) 91–100.
[33] S.-Y. Oh, S.-G. Kang, P.C. Chiu, Degradation of 2,4-dinitrotoluene by persulfate activated with zero-valent iron, Sci. Total. Environ., 408 (2010) 3464–3468.
[34] S. Rodriguez, L. Vasquez, D. Costa, A. Romero, A. Santos, Oxidation of Orange G by persulfate activated by Fe(II), Fe(III) and zero valent iron (ZVI), Chemosphere, 101 (2014) 86–92.
[35] X. Wang, L. Wang, J. Li, J. Qiu, C. Cai, H. Zhang, Degradation of Acid Orange 7 by persulfate activated with zero valent iron in the presence of ultrasonic irradiation, Sep. Purif. Technol., 122 (2014) 41–46.
[36] Y.-H. Hwang, D.-G. Kim, H.-S. Shin, Effects of synthesis conditions on the characteristics and reactivity of nano scale zero valent iron, Appl. Catal., B, 105 (2011) 144–150.
[37] F.D. Snell, C.T. Snell, Colorimetric Methods of Analysis, 3rd ed., 2D. Van Nostrand Company, Toronto, 1959.
[38] APHA, Standard Methods for the Examination of Water and Wastewater, 17th ed., APHA, AWWA, WPCF, American Public Health Association, Washington, D.C., USA, 1989.
[39] Y.-P. Sun, X.-q. Li, J. Cao, W.-x. Zhang, H.P. Wang, Characterization of zero-valent iron nanoparticles, Adv. Colloid Interface Sci., 120 (2006) 47–56.
[40] Z. Fang, J. Chen, X. Qiu, X. Qiu, W. Cheng, L. Zhu, Effective removal of antibiotic metronidazole from water by nanoscale zero-valent iron particles, Desalination, 268 (2011) 60–67.
[41] J. Fan, Y. Guo, J. Wang, M. Fan, Rapid decolorization of azo dye methyl orange in aqueous solution by nanoscale zerovalent iron particles, J. Hazard. Mater., 166 (2009) 904–910.
[42] L. Shi, Y.-M. Lin, X. Zhang, Z.-l. Chen, Synthesis, characterization and kinetics of bentonite supported nZVI for the removal of Cr(VI) from aqueous solution, Chem. Eng. J., 171 (2011) 612–617.
[43] J. Chen, X. Qiu, Z. Fang, M. Yang, T. Pokeung, F. Gu, W. Cheng, B. Lan, Removal mechanism of antibiotic metronidazole from aquatic solutions by using nanoscale zero-valent iron particles, Chem. Eng. J., 181–182 (2012) 113–119.
[44] B.I. Harman, M. Genisoglu, Synthesis and characterization of pumice supported nZVI for removal of copper from waters, Adv. Mater. Sci. Eng., 2016 (2016) 4372136. Available at: http://dx.doi.org/10.1155/2016/4372136.
[45] F. Ghanbari, M. Moradi, M. Manshouri, Textile wastewater decolorization by zero valent iron activated peroxymonosulfate: compared with zero valent copper, J. Environ. Chem. Eng., 2 (2014) 1846–1851.
[46] Y. Ji, C. Ferronato, A. Salvador, X. Yang, J.-M. Chovelon, Degradation of ciprofloxacin and sulfamethoxazole by ferrous-activated persulfate: implications for remediation of groundwater contaminated by antibiotics, Sci. Total. Environ., 472 (2014) 800–808.
[47] Z.-H. Diao, X.-R. Xu, H. Chen, D. Jiang, Y.-X. Yang, L.-J. Kong, Y.-X. Sun, Y.-X. Hu, Q.-W. Hao, L. Liu, Simultaneous removal of Cr(VI) and phenol by persulfate activated with bentonite-supported nanoscale zero-valent iron: reactivity and mechanism, J. Hazard. Mater., 316 (2016) 186–193.
[48] C. Zhu, G. Fang, D.D. Dionysiou, C. Liu, J. Gao, W. Qin, D. Zhou, Efficient transformation of DDTs with persulfate activation by zero-valent iron nanoparticles: a mechanistic study, J. Hazard. Mater., 316 (2016) 232–241.